

OPTICAL FLOW ESTIMATION OF THE HEART MOTION USING LINE PROCESS

Hrvoje Bogunović, Sven Lončarić
Faculty of Electrical Engineering and Computing, University of Zagreb
Unska 3, HR-10000 Zagreb, Croatia
email: hrvoje.bogunovic@fer.hr, sven.loncaric@fer.hr

ABSTRACT

This paper uses line process technique from computer vision to enhance optical flow computation for the problem of cardiac motion estimation. The basic idea is to introduce the line process as a tool for handling discontinuities of the optical flow field. Optical flow showing cardiac motion can then become piecewise smooth instead of globally smooth. Points of interest usually lie on the boundaries of the heart and this method is especially accurate at such points. The general problem is stated as a Bayes estimator and uses MRF framework to encode a priori knowledge. The MAP estimation is found as the minimum of the non-convex energy function using Highest Confidence First (HCF) algorithm. The advantages of HCF algorithm are that it is deterministic and the result is not dependant on the initialization step. The procedure is applied to ECG-gated MR image sequence of the beating heart.

KEY WORDS

Cardiac motion estimation, optical flow, line process, MRF framework, MAP estimation

1 Introduction

Useful information about the cardiac function can be extracted from the motion analysis of the beating heart. Very important aspect of cardiac analysis is motion estimation. Here we try to calculate optical flow from the sequence of MR images of the heart. We shall restrict to 2-D motion estimation i.e. we shall calculate optical flow between two slices at different times. Later research will be focused on applying the algorithm to full volumes of the heart thus calculating 3-D optical flow. Very interesting result was achieved by Song and Leahy [1]. They managed to calculate full 3D optical flow of the beating heart. Same was achieved by Gorce et al. [2]. These methods, which rely on work by Horn and Schunk [3], have the same problem as the original method, which is, the smoothing of the boundaries. Since in computer vision the same problem was successfully tackled by the introduction of line process, we wanted to see what would be the effect of it in the medical imaging. Towards the calculation of full 3-D optical flow, we first wanted to explore the 2-D paradigm. Major effect of line process is that it turns optical flow field from globally smooth to piecewise smooth.

First time line process was used was in paper by Geman and Geman [4]. They used it for image restoration. Later Heitz and Bouthemy [5], and Konrad and Dubois [6] independently implemented line process for motion estimation. Some interesting work with the same topic was later done by Tian and Shah [7].

The rest of the paper is organized as follows. In Section 2 we postulate the problem as a MAP estimation which is solved in Section 3. Results are given in Section 4, and Section 5 concludes the paper.

2 Energy function

Let F be the random field (RF). F has sites placed on a regular grid corresponding to image pixels. Each random variable of the random field F takes a two-dimensional continuous vector $(u(i, j), v(i, j))$ that represents motion vector of that point. Such field is called, the optical flow field. Final configuration of that random field is of primary interest to us. We also introduce random field L . Unlike RF F , RF L has sites placed midway between two pixels. Variables of field L can have binary values i.e. $\{0, 1\}$. Random field L is known as *line process*. $l_h(i, j)$ and $l_v(i, j)$ represent horizontal and vertical line process variables which connect pixels (i, j) to $(i+1, j)$ and (i, j) to $(i, j+1)$ respectively.

The problem is postulated as the Bayes labeling. Our observation of the sequence are spatio-temporal gradients. Observation is marked with d . Gradients are noted by d_x, d_y, d_t . We are trying to find a maximum a posteriori (MAP) solution to our problem.

$$P(F = f^*, L = l^* | d) \geq P(F = f, L = l | d) \quad (1) \\ \forall f \neq f^*, l \neq l^*$$

Using the Bayes rule we may write.

$$P(F = f, L = l | d) = \frac{P(d | F = f, L = l) P(F = f, L = l)}{P(d)} \quad (2)$$

Since denominator is constant, it does not influence the MAP estimation, thus it will be further neglected. Here we can see two factors. First one is called *likelihood probability* and denotes the relationship between our observation and resulting random fields. The brightness constancy constraint is used for the likelihood probability. Random field

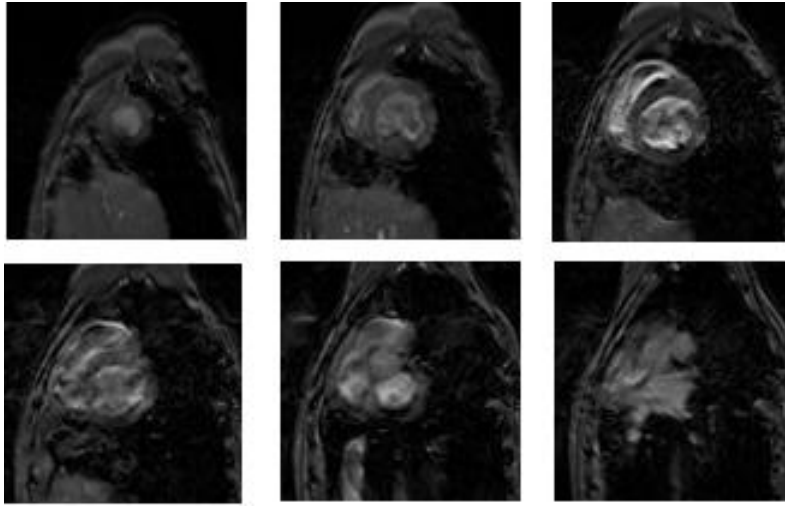


Figure 1. Heart slices no. 3,7,10,12,14,16

L does not depend on that constraint.

$$\begin{aligned}
 P(d|f, l) &= P(d|F = f) = & (3) \\
 &= \exp\left(\frac{1}{2\sigma^2} \sum_i \sum_j (u(i, j)d_x(i, j) + v(i, j)d_y(i, j) \right. \\
 &\quad \left. + d_t(i, j))^2\right)
 \end{aligned}$$

On the other end we have *a priori* probability function. Markov Random Fields (MRF) framework is utilized for displaying prior knowledge. We turn F and L from RF to MRF by defining neighbourhoods and cliques. Thus we obtained coupled MRF. A 4-point neighborhood and cliques up to second order were used. Now we can express prior probability. We can also write $P(F = f, L = l) = P(F = f|L = l)P(L = l)$. $P(F = f|L = l)$ should present interaction between two fields. Typical expression for this is.

$$\begin{aligned}
 P(f|l) &= & (4) \\
 &= \exp\left(-\frac{1}{\beta_f} \sum_i \sum_j [(u_x(i, j)^2 + v_x(i, j)^2)(1 - l_v(i, j)) \right. \\
 &\quad \left. + (u_y(i, j)^2 + v_y(i, j)^2)(1 - l_h(i, j))]\right)
 \end{aligned}$$

Our *a priori* knowledge consists of the fact that motion vectors are not necessarily smooth across the edges of the image. So line process is used to help us signaling potential discontinuity of the motion field. Additionally we need to make a penalty every time line process signals discontinuity because otherwise we would end up with every site of line process having value 1. To make things easier, motion discontinuity should only appear if there is a corresponding edge discontinuity.

As a prerequisite we should first find the spatial edges. That was done using Canny edge detector. If we want the penalty for creating discontinuity outside the corresponding intensity edge to be 10 times higher than if there exists

intensity edge, we would use:

$$\begin{aligned}
 P(l) &= & (5) \\
 &= \exp\left(-\frac{1}{\beta_l} \sum_i \sum_j ((1 - edge_h(i, j)) \cdot 9 \cdot l_h(i, j) + \right. \\
 &\quad \left. l_h(i, j) + (1 - edge_v(i, j)) \cdot 9 \cdot l_v(i, j) + l_v(i, j))\right)
 \end{aligned}$$

It is interesting to note that the output of the edge detector should have values located at the same positions as the line process i.e. midway between pixels. Normal edge detector gives output on a regular grid which corresponds to pixel sites. That is why we had to take orientation of the edge into account. Our implementation of Canny edge detector produced edge always on the brighter side of the real edge that lays between pixels. By moving in the opposite direction from the orientation of the edge by half a pixel, we can come to the actual position of the edge.

When we multiply all the factors, and if we want MAP estimate, we have to minimize the following energy function.

$$\begin{aligned}
 U(f, l|d) &= & (6) \\
 &= \sum_i \sum_j \frac{1}{2\sigma^2} (u(i, j)d_x(i, j) + v(i, j)d_y(i, j) + d_t)^2 \\
 &\quad + \frac{1}{\beta_f} [(u_x(i, j)^2 + v_x(i, j)^2)(1 - l_v(i, j)) + \\
 &\quad + (u_y(i, j)^2 + v_y(i, j)^2)(1 - l_h(i, j))] + \\
 &\quad + \frac{1}{\beta_l} (l_h(i, j) + l_v(i, j))
 \end{aligned}$$

We have three parameters in this equation. if we take

$$\frac{1}{2\sigma^2} = 1 ; \quad \lambda = \frac{\frac{1}{\beta_f}}{\frac{1}{2\sigma^2}} ; \quad \gamma = \frac{\frac{1}{\beta_l}}{\frac{1}{2\sigma^2}}$$

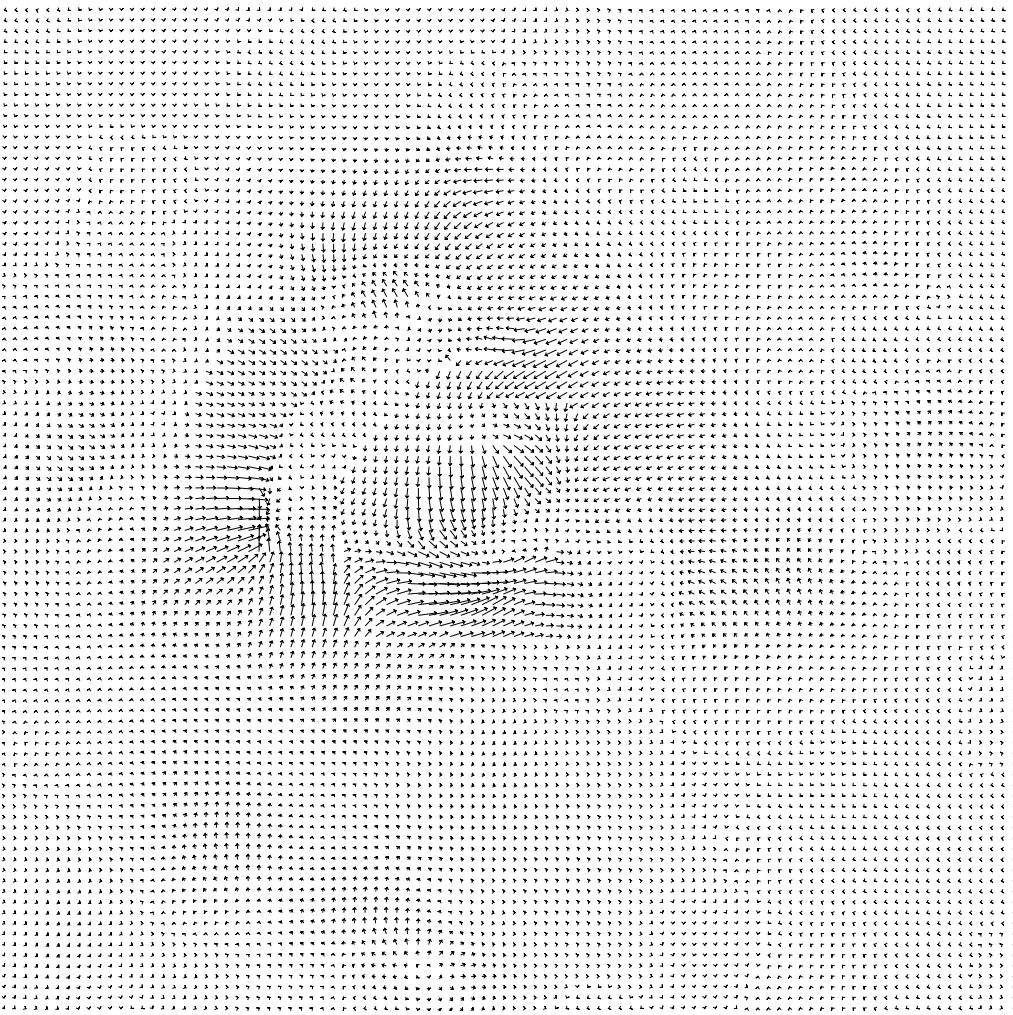


Figure 2. Optical flow for slice no. 10, $\lambda = 30$, $\gamma = 1$

then we have only two parameters. We have not found an efficient way to estimate these parameters so they were chosen *ad hoc*.

We can point out though, what is the threshold needed for the discontinuity to appear. If discontinuity appears energy will rise by γ otherwise it will rise by $\lambda(\text{grad}(\text{vel})^2)$. So the threshold required for the discontinuity to appear will be $\sqrt{\frac{\gamma}{\lambda}}$. If $\text{grad}(\text{vel}) \geq \sqrt{\frac{\gamma}{\lambda}}$ discontinuity will appear otherwise it will not.

3 Energy minimization

Minimization was performed with HCF (Highest Confidence First) algorithm, first presented by Chou and Brown [8]. The good thing about that algorithm is that it does not require accurate initialization of random fields. The energy defined by equation 6 which we have to minimize is non-convex. That means it has multiple minima and any kind of steepest descent algorithm will get trapped into

local minimum too easily. HCF algorithm uses advanced system for site visiting which enables to avoid most of the local minimums.

At the beginning, sites of both fields (F and L) possess label l_0 , meaning uncommitted. Also sites from both fields are treated equally. Every site is visited in order of its stability. Stability presents measure of validity of their current label. At the beginning when all sites are uncommitted the stability shows whether the observation is strong enough at that point for site to know its label. Least stable sites will be visited early since their current label obviously is not valid. Also sites which do not possess a strong observation will be visited the least, when labels of their neighbours will be committed and decision can depend on context.

In such a way HCF is able to evade some local minima. Since it is deterministic results are obtained quite fast. Compared to Simulated Annealing algorithm it is couple of orders of magnitude faster with the results being quite similar.

4 Results

The heart is presented as 16 slices with resolution 100x100. The whole sequence consists of 16 volumes in time. Results will be presented on slice 10 since it depicts the middle slice where left ventricle and myocardium are most visible. We needed three time slices to calculate temporal gradient since we used three-point central difference.

All images were smoothed with Gaussian filter before calculating spatio-temporal derivatives due to strong noise. Typical slices of heart are given in figure 1. The resulting optical flow for slice no. 10 is given in figure 2. Result given by edge detector for slice no. 10 is given in figure 3. Line process field is depicted on figure 4.



Figure 3. Result of Canny edge detector on slice no. 10

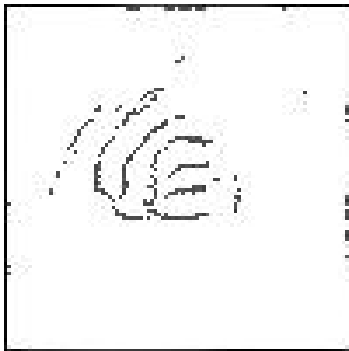


Figure 4. Resulting line process field of slice no. 10

It is visible that only edges of the image surrounding the moving heart produce discontinuity in motion field. That proves that the line process performs well.

The resulting optical flow field needs further validation from the physicians.

In the past major drawback of algorithms based on MRF, was slow execution time. Since processors are becoming faster and faster that drawback is slowly disappearing. We were able to produce the results on Pentium III (933 MHz) processor within 10 seconds.

5 Conclusion

From the results it seems that line process can be valuable in cardiac analysis. Resulting optical flow field is indeed piecewise smooth instead of globally smooth. Additional advantage of line process is that it performs simultaneously with optical flow field. In this way both fields help each other to acquire correct values.

Experiments have shown encouraging results but still require further clinical validation.

The next logical step would be to fully implement 3-D optical flow estimator. The heart is 3-D object undergoing 3-D motion and results obtained in two dimensions cannot present accurate estimate needed for modeling of real heart motion.

6 Acknowledgements

The authors wish to thank Prof. James Duncan for providing us with the ECG-gated MR images of the heart.

References

- [1] S.M. Song, R.M. Leahy, Computation of 3-D Velocity Fields from 3-D Cine CT Images of a Human Heart. *IEEE Transactions on Medical Imaging*, 10(3), 1991, 295–306
- [2] J-M. Gorce, D. Friboulet, I.E. Magnin, Estimation of three-dimensional cardiac velocity fields: assessment of a differential method and application to three-dimensional CT data. *Medical Image Analysis*, 1(3), 1997, 245–261
- [3] B.K.P Horn, B. Schunk, Determining Optical Flow. *Artificial Intelligence*, 17, 1981, 185–203
- [4] S. Geman, D. Geman, Stochastic Relaxation, Gibbs distributions, and the Bayesian restoration of images. *IEEE Transactions on Pattern Analysis and Machine Intelligence*, 6(6), 1984, 721–741
- [5] F. Heitz, P. Bouthemy, Multimodal Estimation of Discontinuous Optical Flow Using Markov Random Fields. *IEEE Transactions on Pattern Analysis and Machine Intelligence*, 15(12), 1993, 1217–1232
- [6] J. Konrad, E. Dubois, Bayesian Estimation of Motion Vector Fields. *IEEE Transactions on Pattern Analysis and Machine Intelligence*, 14(9), 1992, 910–927
- [7] T.Y. Tian, M. Shah, Motion Estimation and Segmentation. *Machine Vision and Applications*, 9, 1996, 32–42
- [8] P.B. Chou, C.M. Brown, The Theory and Practice of Bayesian Image Labeling. *International Journal of Computer Vision*, 4, 1990, 185–210